




A Eurasian avian-like H1N1 swine influenza reassortant virus became pathogenic and highly transmissible due to mutations in its PA gene

Fei Meng^{a,1}, Huanliang Yang^{a,1}, Zhiyuan Qu^a, Yan Chen^a, Yijie Zhang^a, Yaping Zhang^a, Liling Liu^a, Xianying Zeng^a, Chengjun Li^{a,b}, Yoshihiro Kawaoka^{c,d,e,2} , and Hualan Chen^{a,b,2}

Contributed by Yoshihiro Kawaoka; received March 16, 2022; accepted June 18, 2022; reviewed by Amy Vincent Baker, Juergen Richt, and Terrence Tumpey

Previous studies have shown that the Eurasian avian-like H1N1 (EA H1N1) swine influenza viruses circulated widely in pigs around the world and formed multiple genotypes by acquiring non-hemagglutinin and neuraminidase segments derived from other swine influenza viruses. Swine influenza control is not a priority for the pig industry in many countries, and it is worrisome that some strains may become more pathogenic and/or transmissible during their circulation in nature. Our routine surveillance indicated that the EA H1N1 viruses obtained different internal genes from different swine influenza viruses and formed various new genotypes. In this study, we found that a naturally isolated swine influenza reassortant, A/swine/Liaoning/265/2017 (LN265), a representative strain of one of the predominant genotypes in recent years, is lethal in mice and transmissible in ferrets. LN265 contains the hemagglutinin, neuraminidase, and matrix of the EA H1N1 virus; the basic polymerase 2, basic polymerase 1, acidic polymerase (PA), and nucleoprotein of the 2009 H1N1 pandemic virus; and the nonstructural protein of the North American triple-reassortment H1N2 virus. By generating and testing a series of reassortants and mutants, we found that four gradually accumulated mutations in PA are responsible for the increased pathogenicity and transmissibility of LN265. We further revealed that these mutations increase the messenger RNA transcription of viral proteins by enhancing the endonuclease cleavage activity and viral RNA-binding ability of the PA protein. Our study demonstrates that EA H1N1 swine influenza virus became pathogenic and transmissible in ferrets by acquiring key mutations in PA and provides important insights for monitoring field strains with pandemic potential.

swine influenza | H1N1 | Eurasian lineage | PA | transmission | pathogenicity

Influenza A viruses continue to challenge human and animal health. The genome of the influenza virus consists of eight single-strand RNA fragments, including basic polymerase 1 (PB1), basic polymerase 2 (PB2), acidic polymerase (PA), hemagglutinin (HA), nucleoprotein (NP), neuraminidase (NA), matrix (M), and nonstructural protein (NS). This segmented genome allows gene reassortment when different viruses infect the same host cell. Influenza viruses constantly evolve and generate new strains by acquiring mutations and through genetic reassortment. Certain mutations or gene constellations increase the pathogenicity and/or transmissibility of influenza viruses, and such strains may cause severe disease or an influenza pandemic if they jump to naïve humans (1–4). The H1N1, H2N2, and H3N2 subtypes of influenza viruses containing certain gene segments or the entire genome of animal influenza viruses caused influenza pandemics in 1918, 1957, 1968, and 2009 (5, 6). In recent decades, the H5N1, H5N6, H7N7, and H7N9 subtypes of avian influenza viruses have caused severe disease outbreaks in domestic poultry in various countries (7–10). These avian influenza viruses have also caused more than 2,000 human cases of infection, with mortality rates for the H5 and H7N9 human cases of more than 50% and 39%, respectively (11–13). These facts emphasize the threat to human health posed by animal influenza viruses and the importance of carefully monitoring and analyzing field strains for their pandemic potential.

Pigs have been considered as intermediate hosts for the generation of pandemic influenza viruses, since both avian and human influenza viruses can replicate in swine airway epithelial cells (14, 15). Two lineages of H1N1 swine influenza viruses—classical H1N1 viruses and Eurasian avian-like H1N1 (EA H1N1) viruses—have been circulating in pigs since 1918 and 1979, respectively (14, 16). The HA genes of the classical H1N1 viruses and EA H1N1 viruses evolved into different clades and subclades, and the HA genes of the EA H1N1 viruses detected in China belong to the clade 1C.2.3 (17). The classical H1N1 viruses bearing the clade 1A.3.3.2 HA emerged in humans as a reassortant (2009/H1N1)

Significance

Eurasian avian-like H1N1 (EA H1N1) swine influenza viruses have been circulating in pigs in many European and Asian countries and have caused multiple human infections throughout Europe and China. In this study, we found that an EA H1N1 reassortant isolated from pigs in China has become pathogenic in mice and transmissible in ferrets, posing an increased threat to public health. We further found that this EA H1N1 virus obtained these harmful characteristics by accumulating mutations in its acidic polymerase (PA) gene and that the PA gene bearing these mutations was predominant in the 2009/H1N1 viruses in humans and progressively increased in the 2009/H1N1 viruses in swine. Our study emphasizes the importance of monitoring and evaluating the EA H1N1 viruses in pigs for their pandemic potential.

Reviewers: A.V.B., USDA Agricultural Research Service; J.R., Kansas State University; and T.T., Centers for Disease Control and Prevention

The authors declare a competing interest. Y.K. has received unrelated funding support from Daiichi Sankyo Pharmaceutical; Toyama Chemical; Tauns Laboratories, Inc.; Shionogi & Co. Ltd.; Otsuka Pharmaceutical; KM Biologics; Kyoritsu Seiyaku; Shinya Corporation; and Fuji Rebio.

Copyright © 2022 the Author(s). Published by PNAS. This article is distributed under [Creative Commons Attribution-NonCommercial-NoDerivatives License 4.0 \(CC BY-NC-ND\)](https://creativecommons.org/licenses/by-nc-nd/4.0/).

¹F.M. and H.Y. contributed equally to this work.

²To whom correspondence may be addressed. Email: chenhualan@caas.cn or yoshihiro.kawaoka@wisc.edu.

This article contains supporting information online at <http://www.pnas.org/lookup/suppl/doi:10.1073/pnas.2203919119/-DCSupplemental>.

Published August 15, 2022.

and caused the 2009 H1N1 influenza pandemic (5, 18). Influenza virus easily undergoes reassortment in nature, and viruses bearing a similar HA gene may have different NA and internal genes; in this article, we call any H1N1 virus bearing the clade 1C.2.3 HA of EA H1N1 virus origin an “EA H1N1 virus.” Studies indicate that 2009/H1N1 virus possesses HA, NP, and NS genes of classical H1N1 virus origin; PB2 and PA genes of North American avian virus origin; a PB1 gene of human H3N2 virus origin; and NA and M genes of EA H1N1 virus origin (1, 5). It then obtained key mutations in its HA and PB2 genes that promoted its transmissibility (19). The EA H1N1 swine influenza viruses have been detected in pigs in many Eurasian countries (20) and have caused multiple human infections throughout Europe and China (21–31), including two fatal cases (22, 29).

We previously reported that the EA H1N1 swine influenza viruses were predominant in pigs in China, and some of them can transmit in ferrets via respiratory droplets; they can also replicate efficiently in mice, although they are not highly lethal in this animal (3). Our subsequent surveillance indicated that the EA H1N1 viruses obtained different internal genes from different swine influenza viruses and formed different new genotypes (*SI Appendix, Fig. S1*). Viruses of genotype 4 (G5 in Sun et al. [4]), which contain HA, NA, and M from EA H1N1 virus; PB2, PB1, PA, and NP from 2009/H1N1 virus; and NS from North American triple-reassortment H1N2 virus, and genotype 5 (G4 in Sun et al. [4]), which contain HA and NA from EA H1N1 virus; PB2, PB1, PA, NP, and M from 2009/H1N1 virus; and NS from North American triple-reassortment H1N2 virus, dominate in pigs in China, accounting for 42.6% and 53.6%, respectively, of the total EA H1N1 viruses that we isolated from pigs between 2013 and 2019 (*SI Appendix, Fig. S1*). Sun et al. reported that certain EA H1N1 reassortants caused severe disease in pigs (4), implying that some EA H1N1 reassortants may have become more pathogenic to mammals. In the present study, we selected two viruses as model strains and explored the underlying mechanism that makes the EA H1N1 swine influenza virus pathogenic and transmissible in ferrets. We found that gradually accumulated mutations in PA have increased the pathogenicity of EA H1N1 virus in mice and ferrets and that these mutations play a key role in the efficient transmission of the virus in ferrets. Moreover, we revealed the molecular mechanism of PA’s contribution to pathogenicity. Our study provides important information for monitoring field strains with pandemic potential.

Results

Replication and pathogenicity of two EA H1N1 swine influenza viruses in mice. A/swine/Guizhou/828/2016 (H1N1) (GZ828) and A/swine/Liaoning/265/2017 (H1N1) (LN265) are H1N1 viruses that we isolated from pigs during our routine surveillance. Sequence analysis showed that these two viruses have similar genomic components with their HA, NA, and M genes from EA H1N1 viruses; PB2, PB1, PA, and NP genes from 2009/H1N1 viruses; and NS genes from triple-reassortment H1N2 viruses (genotype 4, shown in *SI Appendix, Fig. S1*) (the sequence data have been deposited in the Global Initiative on Sharing Avian Influenza Data; the accession numbers are EPI1987738—EPI1987753). These two viruses share the same gene constellation with the G5 viruses reported by Sun et al. (4) and the G2 viruses reported by H. Li et al. (32). To evaluate the replication of these two viruses in mammals, groups of three BALB/c mice were intranasally (i.n.) inoculated with $10^{6.0}$ 50% egg infectious dose (EID₅₀) of each virus. Mice were

ethanized on day 3 postinfection (p.i.), and their nasal turbinates, lungs, spleen, kidneys, and brain were collected for virus titration. Replication of GZ828 was detected in the nasal turbinates and lungs of mice, whereas LN265 was detected in the turbinates, lungs, spleen, and brain, with titers significantly higher than those in the GZ828-inoculated mice (Fig. 1*A*). To assess pathogenicity, groups of six mice were i.n. inoculated with $10^{2.0}$ to $10^{6.0}$ EID₅₀ of virus and were monitored daily for 2 wk. The 50% mouse lethal dose (MLD₅₀) values of GZ828 and LN265 were 5.5 log₁₀EID₅₀ and 2.5 log₁₀EID₅₀, respectively (Fig. 1*B* and *C*). These results indicate that LN265 replicates much more efficiently and is 1,000-fold more lethal than GZ828 in mice.

The PA gene plays a major role in the difference in pathogenicity between the GZ828 and LN265 viruses in mice. To identify which gene contributes to the pathogenicity difference between these two viruses in mice, we established reverse genetic systems for the GZ828 and LN265 viruses as described previously (33). We then rescued the two wild-type viruses (designated rGZ828 and rLN265), and eight single-gene reassortants using LN265 as the backbone. These reassortants were designated as rLN265-GZ828PB2, rLN265-GZ828PB1, rLN265-GZ828PA, rLN265-GZ828HA, rLN265-GZ828NP, rLN265-GZ828NA, rLN265-GZ828M, and rLN265-GZ828NS, respectively. The replication and MLD₅₀ values of these 10 viruses were evaluated in mice. We found that the replication and pathogenicity of rGZ828 and rLN265 were similar to their wild-type parental viruses (*SI Appendix, Fig. S2* and Fig. 1*D–F*). Seven reassortants—rLN265-GZ828PB2, rLN265-GZ828PB1, rLN265-GZ828HA, rLN265-GZ828NP, rLN265-GZ828NA, rLN265-GZ828M, and rLN265-GZ828NS—replicated in mice with titers in nasal turbinates and lungs similar to those of rLN265-inoculated mice (*SI Appendix, Fig. S2*); their MLD₅₀ values ranged from 2.0 log₁₀EID₅₀ to 2.8 log₁₀ EID₅₀ (Fig. 1*F*). However, the replication titers of rLN265-GZ828PA in the nasal turbinates and lungs of mice were significantly lower than those of rLN265-inoculated mice (Fig. 1*D*), and the pathogenicity of rLN265-GZ828PA was attenuated 10,000-fold compared with rLN265 in mice (MLD₅₀: 6.5 log₁₀EID₅₀ versus 2.5 log₁₀EID₅₀) (Fig. 1*F*). These results indicate that the PA gene is the major contributor to the pathogenicity of LN265 in mice and is required to maintain the lethality of LN265 in mice. To investigate which gene of LN265 would increase the pathogenicity of GZ828, we generated eight single-gene reassortants using GZ828 as the backbone and tested them in mice. We found that the replication titers of rGZ828-LN265PA in the nasal turbinates and lungs of mice were significantly higher than those of rGZ828-inoculated mice (Fig. 1*E*), and the replication titers of rGZ828-LN265HA in the nasal turbinates and lungs of mice were significantly lower than those of rGZ828-inoculated mice. The other six single-gene reassortants replicated in mice similarly to the rGZ828 (*SI Appendix, Fig. S3A*). The pathogenicity of rGZ828-LN265PA was enhanced 1,000-fold compared with rGZ828 in mice (MLD₅₀: 2.5 log₁₀EID₅₀ versus 5.5 log₁₀EID₅₀) (Fig. 1*F*), whereas the MLD₅₀ values of the other seven single-gene reassortants ranged from 5.5 log₁₀EID₅₀ to 6.5 log₁₀EID₅₀ (*SI Appendix, Fig. S3B*).

The PA gene of LN265 significantly increases the polymerase activity of GZ828. The activity of the influenza virus ribonucleoprotein (vRNP) complex, which contains the PB2, PB1, PA, and NP proteins, is important for virus replication and pathogenicity. To investigate whether the difference in pathogenicity between LN265 and GZ828 is associated with the

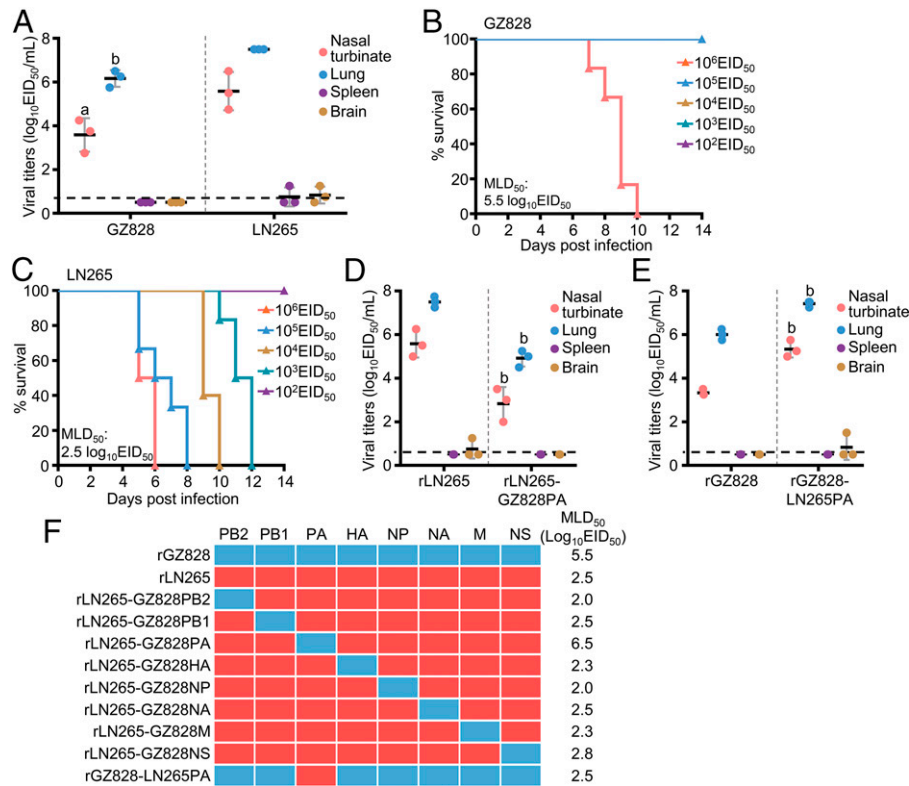


Fig. 1. Replication and pathogenicity of GZ828, LN265, and their reassortants in mice. (A) Viral titers in organs of mice infected with $10^{6.0}$ EID₅₀ of GZ828 or LN265. The organs were collected on day 3 p.i. and titrated in eggs. The data shown are means \pm SD. (B and C) The MLD₅₀ and death patterns of GZ828 and LN265. Groups of six mice were inoculated intranasally with the indicated doses of GZ828 (B) or LN265 (C) and monitored for survival for 14 d. (D and E) Viral titers in organs of mice infected with $10^{6.0}$ EID₅₀ of the indicated virus. The organs were collected on day 3 p.i. and titrated in eggs. The data shown are means \pm SD. (F) The MLD₅₀ values of the rescued rGZ828 and rLN265 and their reassortants. Viral titers in organs and death patterns of reassortants are shown in *SI Appendix, Figs. S2 and S3*. The dashed horizontal lines in panels A, D, and E indicate the lower limit of virus detection. A, $P < 0.05$ and B, $P < 0.01$ compared with the corresponding value of the LN265-(A), rLN265-(D), or rGZ828-(E) infected mice. P values were calculated by using a two-tailed unpaired Student's t test.

polymerase activity of their vRNP complex, we compared the polymerase activity of their vRNP complex using a minigenome assay in human embryonic kidney 293T (HEK293T) cells, as previously described (34). We found that the polymerase activity of the vRNP complex of LN265 was 15.25-fold greater than that of GZ828 (Fig. 2A). We then replaced the PB2, PB1, PA, and NP of the vRNP complex of LN265 individually with the respective proteins of GZ828 and investigated the polymerase activity of the hybrid vRNP complex. We found that the polymerase activity of the hybrid vRNP complex bearing the PB2, PB1, PA, or NP of GZ828 was 116.0%, 56.3%, 5.8%, and 52.6% of that of LN265, respectively. All of these changes were statistically significant, but only the polymerase activity of the hybrid vRNP complex bearing the PA of GZ828 was reduced to a level similar to that of GZ828 (Fig. 2A). The polymerase activity of the hybrid vRNP complex bearing the PB2, PB1, PA, or NP of LN265 was 48.7%, 50.1%, 1,510.0%, and 54.7% of that of GZ828, respectively, indicating that the introduction of the PA of LN265 dramatically increased the polymerase activity of the vRNP of GZ828 to a level similar to that of the vRNP of LN265, whereas the introduction of the PB2, PB1, or NP of LN265 could significantly reduce the polymerase activity of GZ828 (Fig. 2A). These results indicate that PA contributes to the difference in the polymerase activity of the GZ828 and LN265 viruses.

Four amino acids in PA collectively contribute to the difference in the polymerase activity of the vRNP of GZ828 and LN265. The GZ828 and LN265 viruses differ by 13 amino acids in their PA (Fig. 2B). To identify the residue(s) in PA

that may affect polymerase activity, we generated four GZ828/LN265 PA chimeras—chimera 1 (C1), chimera 2 (C2), chimera 3 (C3), and chimera 4 (C4)—and tested the polymerase activity of vRNPs containing each of these PA chimeras and the PB2, PB1, and NP of GZ828. The polymerase activity of the vRNP complex bearing C1 (which contains the N-terminal 331 residues of LN265PA), C3 (which contains the C-terminal 97 residues of LN265PA), and C4 (which contains both the N-terminal 331 residues and the C-terminal 97 residues of LN265PA) was significantly higher than that of GZ828 (Fig. 2C), whereas the polymerase activity of vRNP bearing C2 (which contains residues 332–618 of LN265PA) was similar to that of GZ828 (Fig. 2C). These results indicate that the N-terminal 331 residues and C-terminal 97 residues of the PA of LN265 are important for the high polymerase activity of the vRNP of LN265.

The N-terminal 331 residues and C-terminal 97 residues of GZ828 and LN265 differed by eight amino acids at positions 100, 120, 228, 256, 321, 330, 639, and 643 (Fig. 2B). To find out which amino acid contributes to polymerase activity, we generated eight substitutions in the PA of GZ828—GZ828PA-V100I, GZ828PA-V120I, GZ828PA-S228N, GZ828PA-Q256K, GZ828PA-N321K, GZ828PA-I330V, GZ828PA-A639T, and GZ828PA-R643K—and tested the polymerase activity of the vRNPs bearing each of these PA mutants and the PB2, PB1, and NP of GZ828 in HEK293T cells. We found that five substitutions in PA—V100I, V120I, N321K, I330V, and A639T—increased the polymerase activity by 1.73- to 4.16-fold, whereas the other three substitutions (i.e., S228N, Q256K, and R643K) did not alter the polymerase activity (*SI Appendix, Table S1*).

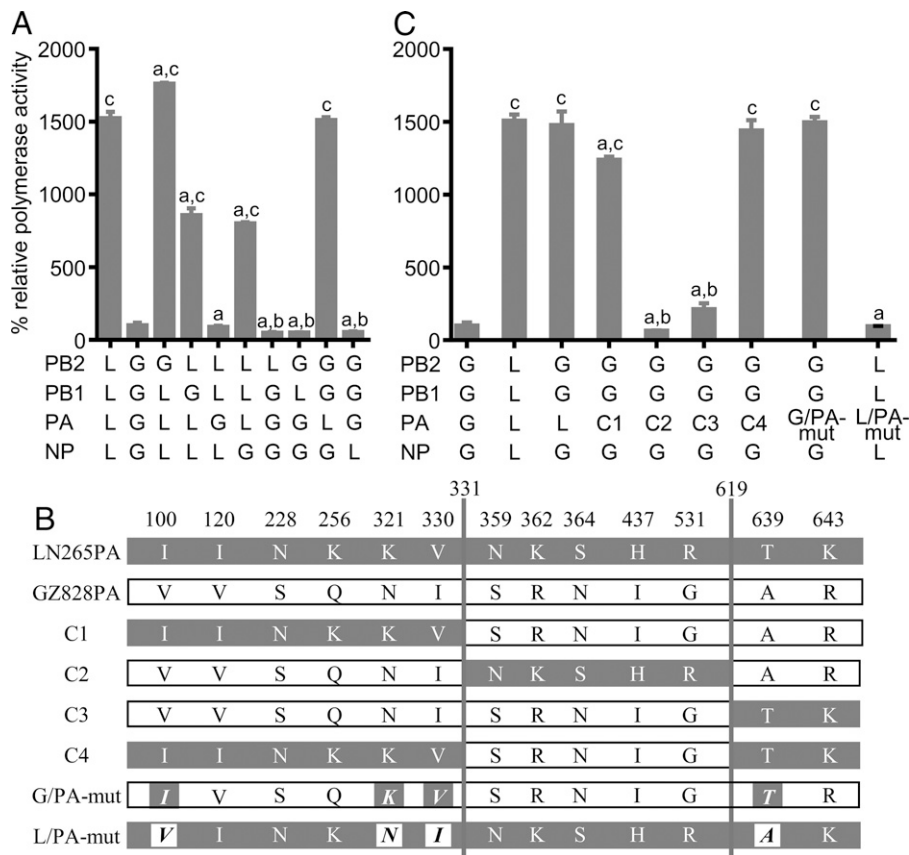


Fig. 2. The gene and key amino acids that contribute to the difference in the polymerase activity of GZ828 and LN265. (A) Polymerase activity of the vRNP complex of GZ828, LN265, and their eight single-gene-segment hybrids. Values shown are means \pm SD of three independent experiments and are standardized to those of GZ828. The chart below shows the parent virus origin of the vRNP complex. Segments derived from GZ828 and those derived from LN265 are denoted by G and L, respectively. (B) The amino acid differences between the PA protein of GZ828 and LN265 are shown as single letters with their positions numbered at the top, and the mutated amino acids are shown in boldface italic type. Four chimeric PA proteins (C1 to C4) bear different parts of the PA of GZ828 and LN265 as indicated. G/PA-mut is the PA of GZ828 bearing the four indicated mutations, and L/PA-mut is the PA of LN265 bearing the four indicated mutations. Amino acid abbreviations: I, Ile; K, Lys; V, Val; T, Thr; N, Asn; A, Ala; S, Ser; H, His; R, Arg; Q, Gln; G, Gly. (C) Polymerase activity of the vRNP complex of GZ828, LN265, and their PA chimeras or mutants. Data shown in panels A and C are means \pm SD of three independent experiments. a, $P < 0.001$ compared with the values of the vRNP of LN265; b, $P < 0.05$; c, $P < 0.001$ compared with the values of the vRNP of GZ828. P values were calculated by using a two-tailed unpaired Student's t test.

These results indicate that single mutations in the PA protein have a limited effect on polymerase activity. We therefore generated 26 mutants of GZ828PA covering all of the possible mutation combinations of V100I, V120I, N321K, I330V, and A639T and tested their contribution to the polymerase activity (*SI Appendix, Table S1*). We found that the polymerase activity of vRNP containing PA bearing four substitutions (V100I, N321K, I330V, and A639T) (designated G/PA-mut) was 14.97-fold higher than that of GZ828 and was similar to that of the vRNP of LN265PA (Fig. 2C), whereas the polymerase activity of the vRNP containing PA with the other 25 mutation combinations was 2.3- to 13.4-fold higher than that of GZ828 (*SI Appendix, Table S1*). To investigate whether reverse mutation of these four amino acids could reduce the polymerase activity of the vRNP of LN265, we introduced I100V, K321N, V330I, and T639A into the PA of LN265 (designated L/PA-mut). We found that the polymerase activity of the vRNP of LN265 that contained L/PA-mut was 16.1-fold lower than that of LN265 (Fig. 2C and *SI Appendix, Table S1*). These results indicate that the four amino acids at positions 100, 321, 330, and 639 in PA synergistically affect the polymerase activity of GZ828 and LN265.

Four amino acids in PA collectively contribute to the difference in the pathogenicity of GZ828 and LN265 in mice. To further investigate whether these four mutations in PA contribute to

the pathogenicity difference between GZ828 and LN265, we generated five mutants of LN265 by introducing the mutations I100V, K321N, V330I, and T639A into its PA, both individually and all four together; these mutants were designated rLN265-PA/I100V, rLN265-PA/K321N, rLN265-PA/V330I, rLN265-PA/T639A, and rLN265-PA/mut, respectively. We also generated five mutants of GZ828 by introducing the mutations V100I, N321K, I330V, and A639T into its PA, both individually and all four together; these mutants were designated rGZ828-PA/V100I, rGZ828-PA/N321K, rGZ828-PA/I330V, rGZ828-PA/A639T, and rGZ828-PA/mut, respectively. The replication and pathogenicity of the mutants were evaluated in mice. We found that the viral titers in the nasal turbinates and/or lungs of mice inoculated with the mutants rLN265-PA/I100V, rLN265-PA/K321N, rLN265-PA/V330I, rLN265-PA/T639A, or rLN265-PA/mut were significantly lower than those in rLN265-inoculated mice (Fig. 3A), and the viral titers in the nasal turbinates and lungs of mice inoculated with the mutants rGZ828-PA/V100I, rGZ828-PA/N321K, rGZ828-PA/I330V, rGZ828-PA/A639T, or rGZ828-PA/mut were significantly higher than those in rGZ828-inoculated mice (Fig. 3B). According to the MLD₅₀ values, the pathogenicity of rLN265-PA/I100V, rLN265-PA/K321N, rLN265-PA/V330I, rLN265-PA/T639A, and rLN265-PA/mut was attenuated by 100-fold, 16-fold, 10-fold, 63-fold, and 7,943-fold, respectively, compared with

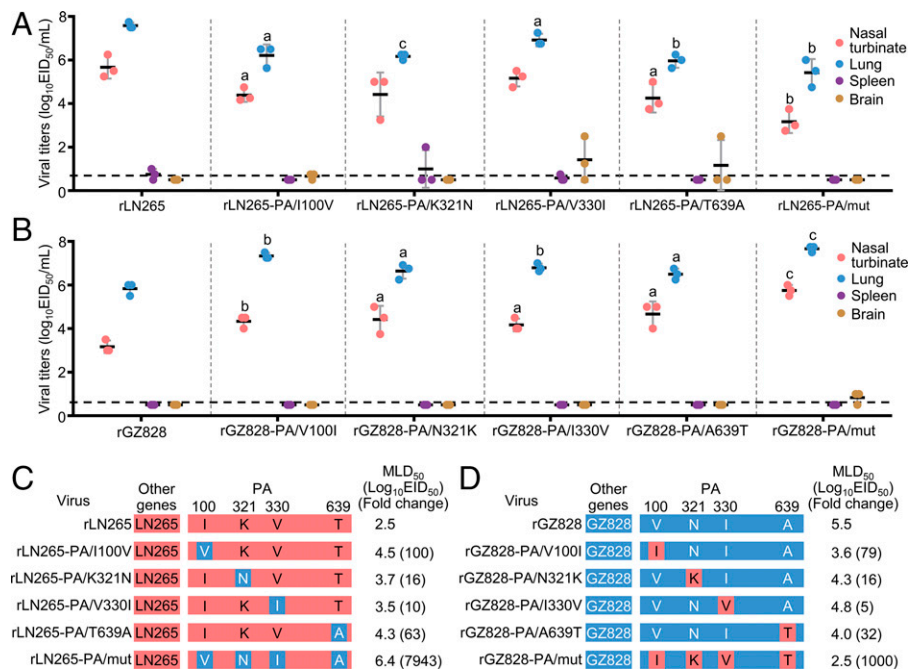


Fig. 3. Replication and pathogenicity of rGZ828, rLN265, and their PA mutants in mice. (A, B) Viral titers in organs of mice infected with $10^{6.0}$ EID₅₀ of the indicated virus. The organs were collected on day 3 p.i. and titrated in eggs. The data shown are means \pm SD. a, $P < 0.05$; b, $P < 0.01$; and c, $P < 0.001$ compared with the corresponding value of the rLN265- (A) or rGZ828-infected mice (B). (C) The MLD₅₀ of rLN265 and its PA mutants. (D) The MLD₅₀ of rGZ828 and its PA mutants. The amino acid differences in PA between LN265 and GZ828 are shown as single letters with the positions numbered at the top in panels C and D. The mutated amino acids were highlighted. Amino acid abbreviations: I, Ile; K, Lys; V, Val; T, Thr; N, Asn; A, Ala.

that of rLN265 (Fig. 3C and *SI Appendix, Fig. S4*), and the pathogenicity of rGZ828-PA/V100I, rGZ828-PA/N321K, rGZ828-PA/I330V, rGZ828-PA/A639T, and rGZ828-PA/mut was enhanced by 79-fold, 16-fold, 5-fold, 32-fold, and 1,000-fold, respectively, compared with that of rGZ828 (Fig. 3D and *SI Appendix, Fig. S4*). Pathological studies were performed on lung samples from mice that were infected with rLN265, rLN265-PA/mut, rGZ828, or rGZ828-PA/mut. The lungs of the rLN265-infected mice and rGZ828-PA/mut-infected mice showed severe bronchopneumonia and interstitial pneumonia (*SI Appendix, Fig. S5 A and G*); viral antigen-positive signals were detected in the epithelial cells of the bronchus and macrophages, and also in the alveolar epithelial cells (*SI Appendix, Fig. S5 B and H*). In contrast, the lungs of the rLN265-PA/mut-infected mice and the rGZ828-infected mice showed mild inflammation (*SI Appendix, Fig. S5 C and E*), and viral antigen-positive signals were mainly detected in the epithelial cells of the bronchus and macrophages (*SI Appendix, Fig. S5 D and F*). These studies demonstrate that these four amino acids in PA collectively contribute to the difference in pathogenicity between GZ828 and LN265 in mice.

The four amino acids (100I, 330V, 321K, and 639T) in PA play a key role in the transmissibility of rLN265 and rGZ828-PA/mut in ferrets. Efficient transmission via respiratory droplets is one of the prerequisites for a respiratory virus to cause a pandemic, and ferrets have been widely used as a model animal for evaluating the transmissibility of respiratory viruses, including influenza viruses and coronaviruses (35–37). To investigate whether the four amino acids in PA identified above affect transmissibility, we tested the replication and respiratory droplet transmission of rLN265, rGZ828, rLN265-PA/mut, and rGZ828-PA/mut in ferrets.

The ferrets were euthanized on day 4 after infection with $10^{6.0}$ EID₅₀ of the test virus, and their organs were collected for virus titration in eggs. Pathological studies were also performed on the lung samples. Macroscopic lesions in the lungs and focal dark red consolidations were observed in the lobes of

ferrets inoculated with rLN265 or rGZ828-PA/mut (Fig. 4A and D) but not in the lungs of ferrets inoculated with rGZ828 or rLN265-PA/mut (Fig. 4B and C). The lungs of the rLN265-infected ferrets and rGZ828-PA/mut-infected ferrets showed severe bronchopneumonia (Fig. 4E and H), whereas mild inflammation was observed in the lungs of the rGZ828-infected ferrets and rLN265-PA/mut-infected ferrets (Fig. 4F and G). Viral antigen was detected in lung samples of animals infected with any of the four viruses, and we did not see any clear difference in tissue tropism (Fig. 4I–L).

Ferret organs were also collected for virus titration in embryonated eggs. The rLN265 and rGZ828-PA/mut viruses were found to replicate to similar levels in the nasal turbinate, soft palate, tonsil, trachea, and all of the lung lobes tested (Fig. 5A and D); although rGZ828 and rLN265-PA/mut also replicated well in the nasal turbinate, soft palate, tonsil, and trachea of ferrets, they were not detected in some of the ferret lung lobes (Fig. 5B and C). The rGZ828 and rGZ828-PA/mut were not detected in the brain of any ferret (Fig. 5C and D), but rLN265 and rLN265-PA/mut viruses were detected in the brain of one ferret (Fig. 5A and B). We speculate that rLN265 and rLN265-PA/mut may have entered the brain through the olfactory bulbs, because high viral titers were detected in the nasal turbinates of the ferrets infected with these two viruses (Fig. 5A and B).

To test the transmission of these viruses, groups of three ferrets, housed separately in solid stainless-steel cages within an isolator, were inoculated with $10^{6.0}$ EID₅₀ of test virus. Twenty-four hours later, three naïve ferrets were placed in adjacent cages as exposed animals. We collected nasal washes from the inoculated ferrets on days 2, 4, 6, 8, and 10 p.i. and from the exposed ferrets on days 1, 3, 5, 7, 9, 11, and 13 postexposure (p.e.) for detection of virus shedding. The body weight of each ferret was recorded after the sample was collected each time, and serum samples were collected from all animals on day 21 p.i. for HA inhibition antibody detection. Virus was detected from the nasal washes of all three animals that were

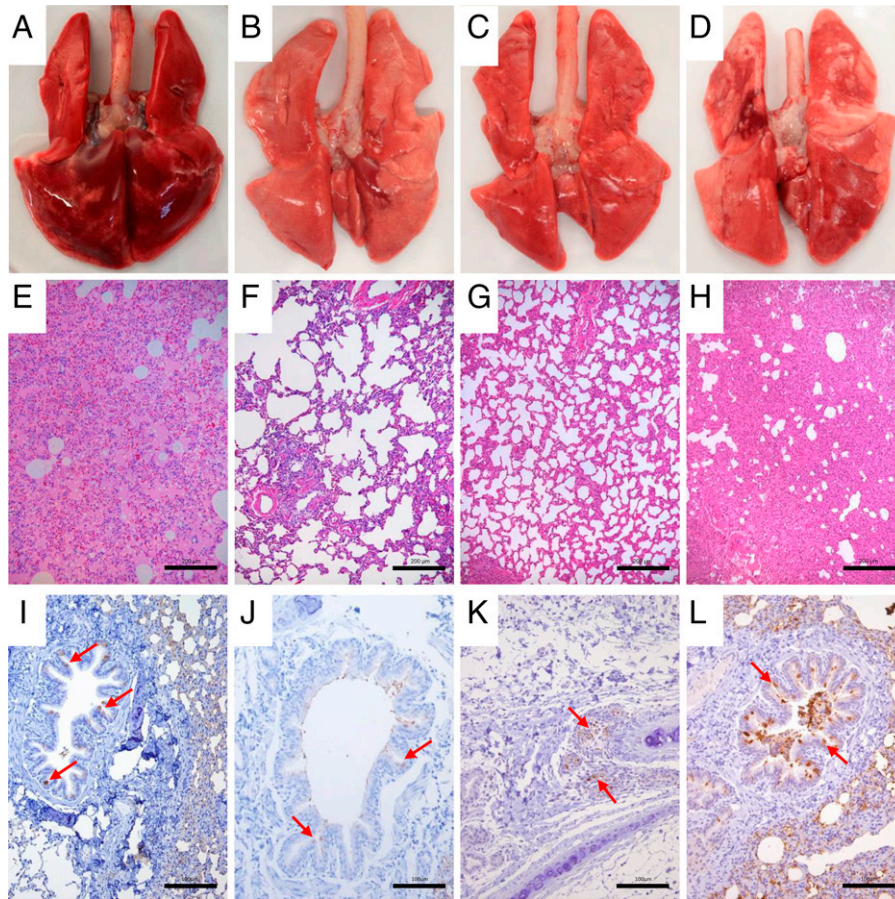


Fig. 4. Lung lesions caused by rLN265, rGZ828, and their PA mutants in ferrets. (A) Macroscopic lesions observed in the lungs of an rLN265-inoculated ferret. The caudal lobes failed to collapse and are mottled with a number of dark-red, edematous, swollen patches. (B) Macroscopic lesions observed in the lungs of an rLN265-PA/mut-inoculated ferret. Small areas of dark-red discoloration can be seen in the right cranial and caudal lobes. (C) No obvious macroscopic lesions observed in the lungs of an rGZ828-inoculated ferret. (D) Macroscopic lesions observed in the lungs of an rGZ828-PA/mut-inoculated ferret. Areas of dark-red discoloration can be seen in the left cranial and right caudal lobes. (E) The lungs of ferrets inoculated with rLN265 virus show severe pathological lesions. Most of the alveoli are dilated and filled with eosinophilic serous exudates with macrophages. Pneumocyte proliferation and mild alveolar wall capillary congestion are also visible. (F and G) Only mild histopathological changes in the lungs of rLN265-PA/mut- and rGZ828-inoculated ferrets. (H) Alveolar epithelial hyperplasia accompanied by numerous inflammatory cell infiltrates resulted in considerable alveolar diaphragm widening in the lungs of an rGZ828-PA/mut-inoculated ferret. Viral antigen (arrow) was detected in the epithelial cells of the bronchus by means of immunohistochemical staining in the lungs of rLN265-inoculated ferrets (I), rLN265-PA/mut-inoculated ferrets (J), and rGZ828-PA/mut-inoculated ferrets (L). Viral antigen (arrow) was detected in the glands of the lungs of rGZ828-inoculated ferrets (K) (Scale bar, [E–H], 200 μ m. Scale bar, [I–L], 100 μ m).

directly inoculated with any of the four viruses (Fig. 5 E–H); virus was detected from the nasal washes of one ferret that was exposed to the rLN265-PA/mut-inoculated animals, two ferrets that were exposed to rGZ828-PA/mut-inoculated animals, and all three ferrets that were exposed to the rLN265-inoculated animals; virus was not detected from the nasal washes of any ferret that was exposed to the rGZ828-inoculated animals (Fig. 5 E–H). All of the inoculated ferrets, the rLN265- and the rGZ828-PA/mut-exposed ferrets, and one of the three rLN265-PA/mut-exposed ferrets seroconverted (Fig. 5 I, J, and L), but none of the rGZ828-exposed ferrets seroconverted (Fig. 5K). The ferrets infected with rLN265 experienced a loss of up to 19% of their body weight (Fig. 5M), whereas the ferrets infected with rLN265-PA/mut, rGZ828, and rGZ828-PA/mut lost less than 10% of their body weight (Fig. 5 N–P). These results indicate that the four amino acids 100I, 321K, 330V, and 639T in PA are critical for the pathogenicity and efficient transmission of LN265 in ferrets, and the substitution of these four amino acids with 100V, 321N, 330I, and 639A in PA reduces the transmissibility of LN265 in ferrets. Introducing these four mutations in PA of GZ828 increases the transmissibility of GZ828 in ferrets; however, the kinetics of transmission of rGZ828-PA/mut differs from those of rLN265.

The four amino acid substitutions in PA affect the transcription of viral proteins.

During influenza virus replication, both complementary RNA (cRNA) and messenger RNA (mRNA) are synthesized from the viral RNA (vRNA) templates. The cRNAs serve as templates for vRNA replication, whereas the mRNAs guide the synthesis of viral proteins. As a component of the vRNP complex, PA is involved in the process of vRNA replication and mRNA transcription. Which step is affected by the four amino acid substitutions in PA? To answer this question, we constructed a vRNA-encoding plasmid, pPolI-vRNA, containing the full-length sequence of the luciferase reporter gene with the upstream 5' noncoding sequence and the downstream 3' noncoding sequence of the NP gene (Fig. 6A). HEK293T cells were cotransfected with pPolI-vRNA and pCAGGS-GZ828PB2, pCAGGS-GZ828PB1, pCAGGS-GZ828NP, and pCAGGS-GZ828PA or pCAGGS-G/PA-mut. Cell lysates were collected at 6 h, 12 h, and 24 h posttransfection (hpt), respectively, and the cRNA, vRNA, and mRNA levels of the luciferase gene were quantified using qRT-PCR. No significant difference was detected in the cRNA and vRNA levels between the two groups (Fig. 6 B and C), whereas the mRNA level in the cells transfected with plasmids containing pCAGGS-G/PA-mut was 1.6-, 13.1-, and 48.2-fold higher than that in the

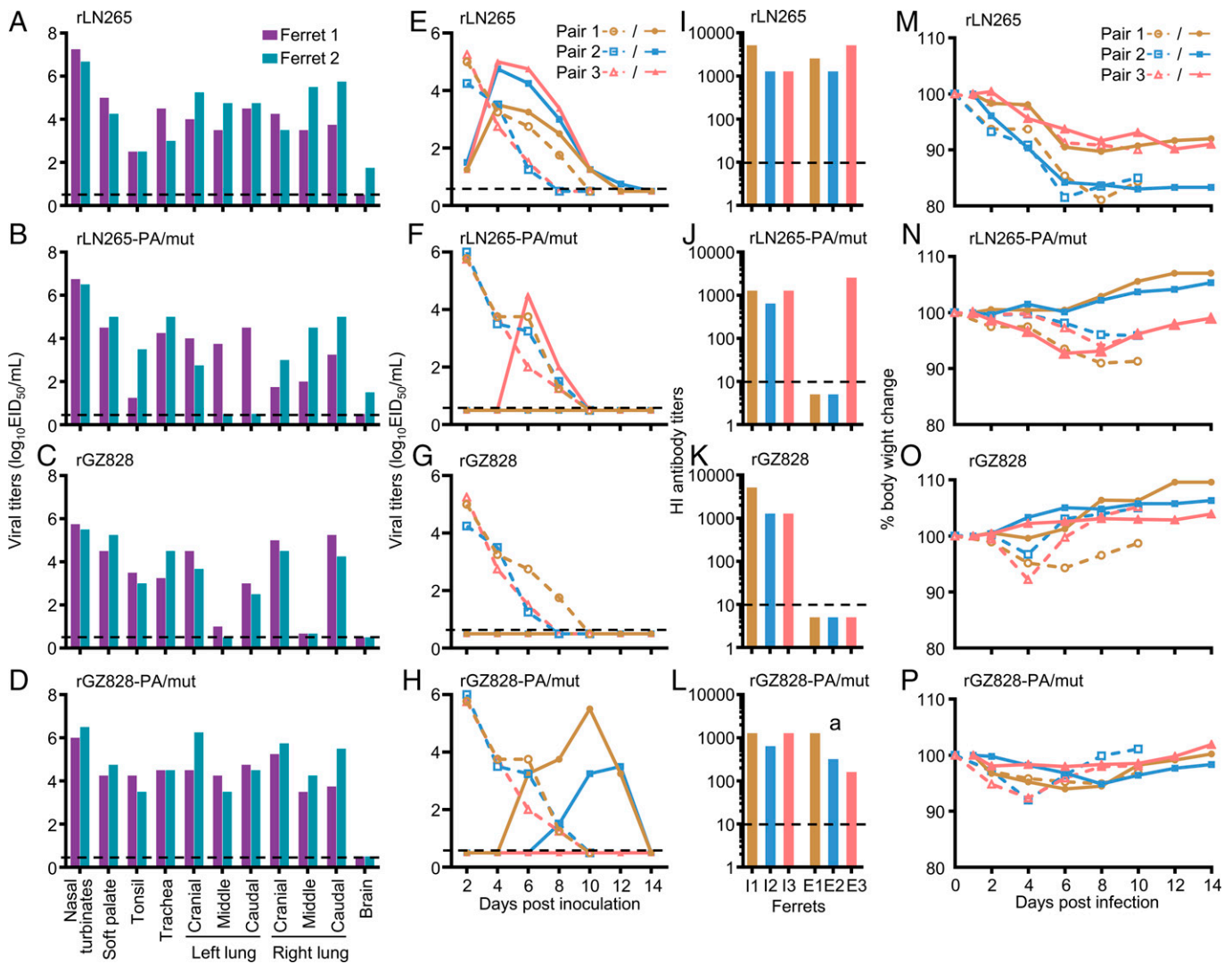


Fig. 5. Replication and respiratory droplet transmission of rLN265, rGZ828, and their PA mutants in ferrets. To evaluate virus replication, groups of two ferrets were inoculated i.n. with $10^{6.0}$ EID₅₀ of rLN265 (A), rLN265-PA/mut (B), rGZ828 (C), or rGZ828-PA/mut (D), and the indicated organs from each ferret were collected on day 4 p.i. for virus titration in eggs. For the transmission study, groups of three ferrets were inoculated intranasally with $10^{6.0}$ EID₅₀ of rLN265 (E), rLN265-PA/mut (F), rGZ828 (G), or rGZ828-PA/mut (H); 24 h later, three naïve ferrets were placed individually in an adjacent cage. Nasal washes were collected from all ferrets at the indicated time points for virus detection. Seroconversion of the rLN265- (I), rLN265-PA/mut- (J), rGZ828- (K), and rGZ828-PA/mut- (L) inoculated and exposed animals was confirmed by use of an HA inhibition test. a, $P < 0.001$ compared with the values of rGZ828 (L) compared with (K). The body weight changes of rLN265- (M), rLN265-PA/mut- (N), rGZ828- (O), and rGZ828-PA/mut- (P) inoculated and exposed animals in the transmission study (Color bar, [A–D] and [I–L], value from an individual animal). The dashed lines and the solid lines in (E–H) and (M–P) indicate the values from the inoculated animals and the exposed animals, respectively. The horizontal dashed black lines indicate the lower limit of detection.

cells transfected with plasmids containing pCAGGS-GZ828PA at 6, 12, and 24 hpt, respectively (Fig. 6D). When we performed similar experiments using the plasmids pCAGGS-LN265PB2, pCAGGS-LN265PB1, pCAGGS-LN265NP, and pCAGGS-LN265PA or pCAGGS-L/PA-mut, we found that the mRNA level in the cells transfected with plasmids containing pCAGGS-L/PA-mut was 1.46-, 9.17-, and 38.5-fold higher than that in the cells transfected with plasmids containing pCAGGS-LN265PA at 6, 12, and 24 hpt, respectively, but no significant difference was detected in the cRNA and vRNA levels between the two groups (Fig. 6F, G, H). We also measured the reporter gene expression levels in these cells and found that the luciferase activity in the cells transfected with plasmids containing pCAGGS-G/PA-mut was 4.8-fold and 15.7-fold higher than that in cells transfected with plasmids containing pCAGGS-GZ828PA at 12 and 24 hpt, respectively (Fig. 6E), and the luciferase activity in the cells transfected with plasmids containing pCAGGS-L/PA-mut was 3.3-fold and 16.2-fold lower than that in cells transfected with plasmids containing pCAGGS-LN265PA at 12 and

24 hpt, respectively (Fig. 6J). These results demonstrate that the four amino acids at positions 100, 321, 330, and 639 in PA affect mRNA transcription but not vRNA replication in the virus life cycle.

The substitutions N321K and I330V in the PA of GZ828 increase its vRNA-binding ability.

The viral polymerases need to bind to the 3' and 5' ends of the vRNA to initiate mRNA transcription, and the binding ability affects the efficiency of mRNA transcription (38–41). The four amino acids mentioned above are in the vRNA-binding domains of PA (42, 43) (Fig. 6J). We therefore investigated whether any of the four amino acids affect the binding of PA to vRNA. To this end, we generated a 300-nt model vRNA (Fig. 6K), containing the conserved 3' and 5' ends and part of the NP gene of GZ828. The model vRNA was incubated at 37 °C for 4 h with a similar amount of PA protein purified from pCAGGS-GZ828PA/V100I-, pCAGGS-GZ828PA/N321K-, pCAGGS-GZ828PA/I330V-, pCAGGS-GZ828PA/A639T-, pCAGGS-G/PA-mut-, pCAGGS-GZ828PA-, and

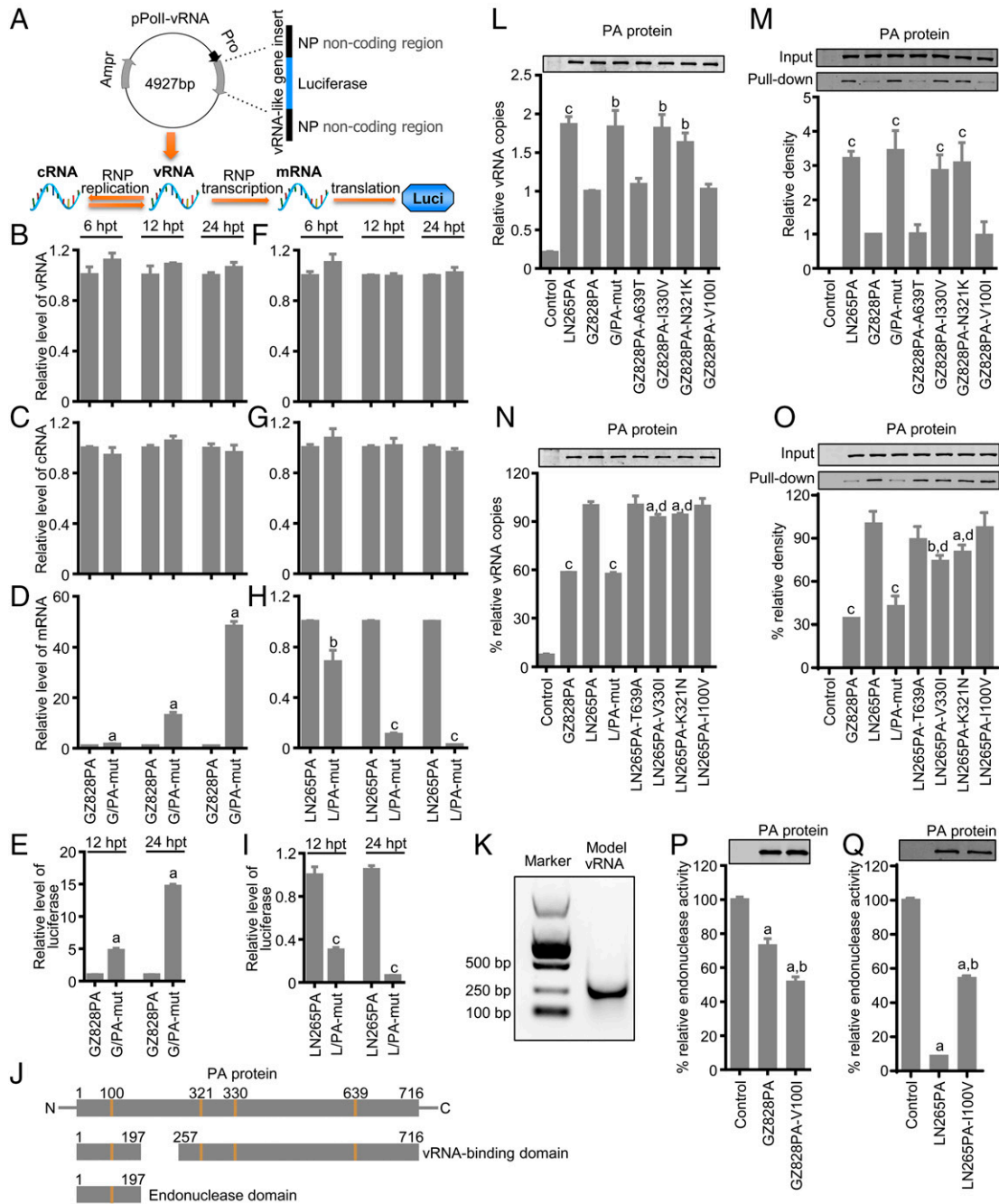


Fig. 6. The mechanism by which key mutations in PA enhance the pathogenicity and transmission of EA H1N1 virus. (A) Schematic depiction of the minigene assay. Luciferase gene bearing the conserved 5' and 3' end sequences of influenza virus RNA was inserted into pPoll plasmid, and the resultant plasmid, designated pPoll-vRNA, was used to evaluate the vRNA, cRNA, and mRNA levels in cells cotransfected with different vRNP plasmids. (B) The vRNA, (C) cRNA, and (D) mRNA level of the luciferase gene, and (E) the relative luciferase activity of HEK293T cells-transfected pRL-TK; pPoll-vRNA; plasmids expressing PB2, PB1, and NP of GZ828; and a plasmid expressing PA of GZ828 or G/PA-mut. (F) The vRNA, (G) cRNA, and (H) mRNA level of the luciferase gene, and (I) the relative luciferase activity of HEK293T cells transfected with pRL-TK; pPoll-vRNA; plasmids expressing PB2, PB1, and NP of LN265; and a plasmid expressing PA of LN265 or L/PA-mut. The levels of vRNA, cRNA, and mRNA were quantified using qPCR and the luciferase activity was determined with a GloMax 96 microplate luminometer at the indicated time (hour) posttransfection (hpt). Data shown are means \pm SD of three independent experiments, normalized to the mRNA of GAPDH. a, $P < 0.001$ compared with the corresponding value of the wild-type GZ828PA group. b, $P < 0.01$. c, $P < 0.001$ compared with the corresponding value of the LN265PA group. P values were determined by using a two-tailed unpaired Student's t test. (J) Schematic depiction of the different domains of the PA protein. (K) A 300-nt model vRNA synthesized in vitro by the T7 promoter. (L) The vRNA bound by LN265PA, GZ828PA, and its different mutants. The bound vRNAs were quantified using qRT-PCR. (M) The wild-type LN265PA, GZ828PA, and its mutated protein pulled down by vRNA. The density of each band of pulled-down PA protein was scaled by using ImageJ software. Values in (L) and (M) are normalized to that of wild-type GZ828PA. (N) The vRNA bound by GZ828PA, LN265PA, and its different mutants. The bound vRNAs were quantified using qRT-PCR. (O) The wild-type GZ828PA, LN265PA, and its mutated protein pulled down by vRNA. The density of each band of pulled-down PA protein was scaled by using ImageJ software. Values in (N) and (O) are normalized to that of wild-type LN265PA. The data shown are means \pm SD of three experiments; the bars show the SDs. a, $P < 0.05$; b, $P < 0.01$; c, $P < 0.001$ compared with the corresponding value of the GZ828PA group (L and M) or LN265PA group (N and O). d, $P < 0.001$ compared with the corresponding value of the GZ828PA group (N and O). (P) The endonuclease activity of GZ828PA and GZ828PA-V100I. The model vRNA that was not cleaved in the reaction was quantified using qRT-PCR. The data shown are means \pm SD of three experiments. a, $P < 0.001$ compared with the value of the negative control group. b, $P < 0.01$ compared with the value of the GZ828PA group. (Q) The endonuclease activity of LN265PA and LN265PA-I100V. a, $P < 0.001$ compared with the value of the negative control group. b, $P < 0.001$ compared with the value of the LN265PA group. P values were determined by using a two-tailed unpaired Student's t test.

pCAGG-LN265PA–transfected HEK293T cells. The vRNA bound by these PA proteins was quantified using qRT-PCR as described previously (40). We found that the amount of vRNA bound by LN265PA, GZ828PA-N321K, GZ828PA-I330V, and G/PA-mut was, respectively, 1.86-fold, 1.63-fold, 1.82-fold, and 1.83-fold greater than that bound by the GZ828PA protein, whereas the amount of vRNA bound by GZ828PA-V100I and GZ828PA-A639T was comparable to that bound by the GZ828PA protein (Fig. 6L). To verify these results, we performed an RNA protein pull-down assay. We found that the amount of LN265PA, GZ828PA-N321K, GZ828PA-I330V, and G/PA-mut protein pulled down by vRNA was, respectively, 3.21-fold, 3.08-fold, 2.85-fold, and 3.44-fold greater than the amount of GZ828PA protein pulled down by vRNA (Fig. 6M). In contrast, the amount of GZ828PA-V100I and GZ828PA-A639T protein pulled down by the vRNA was comparable to the amount of GZ828PA protein pulled down by vRNA (Fig. 6M). These results indicate that the mutations N321K and I330V, but not V100I or A639T, in the PA of GZ828 enhance its vRNA-binding ability.

To further investigate how these amino acids contribute to the vRNA-binding ability of LN265PA, we performed similar tests with the PA proteins expressed by plasmids pCAGGS-LN265PA, pCAGGS-LN265PA/I100V, pCAGGS-LN265PA/K321N, pCAGGS-LN265PA/V330I, pCAGGS-LN265PA/T639A, pCAGGS-GZ828PA, or pCAGGS-L/PA-mut. We found that the amount of vRNA bound by LN265PA-I100V and LN265PA-T639A was comparable to that bound by the LN265PA protein, whereas the amount of vRNA bound by LN265PA-K321N, LN265PA-V330I, L/PA-mut, and GZ828PA was, respectively, 94.1%, 92.4%, 57.3%, and 58.4% of that bound by the LN265PA protein (Fig. 6M). In the RNA protein pull-down assay, we found that the amount of LN265PA-K321N, LN265PA-V330I, L/PA-mut, and GZ828PA protein pulled down by vRNA was, respectively, 80.2%, 73.9%, 42.4%, and 34.2% of the LN265PA protein pulled down by vRNA, whereas there was no significant difference between the amount of LN265PA-I100V or LN265PA-T639A protein and the amount of LN265PA protein pulled down by vRNA (Fig. 6O). These results indicate that the residues at positions 321 and 330, but not 100 or 639, in PA affect the vRNA-binding ability of these EA H1N1 viruses. Of note, a single mutation of N321K or I330V could increase the vRNA-binding ability of GZ828PA to the same level as that of LN265PA, but a single mutation of K321N or V330I could not decrease the vRNA-binding ability of LN265PA to the same level as that of GZ828PA, suggesting that the effect on vRNA-binding of amino acids 321K and 330V in PA may be compensatory.

The amino acid at position 100 in PA affects its endonuclease activity. Viral mRNA transcription is initiated by a 5' capped RNA primer, which is cleaved from host pre-mRNAs by viral PA protein (38). The amino acid at position 100 is in the endonuclease domain of PA (44) (Fig. 6J); therefore, we investigated whether the mutation V100I affects the endonuclease activity of GZ828PA. The 300-nt model vRNA we described earlier contains the conserved 3' and 5' ends and forms a pan-handle structure that could be recognized and cleaved by the endonuclease domain of PA (44). We therefore used it to measure the endonuclease activity of PA proteins that were purified from pCAGGS-GZ828PA– or pCAGGS-GZ828PA/V100I–transfected HEK293T cells. The model vRNA was incubated with a similar amount of purified GZ828PA or GZ828PA/V100I at 37 °C for 40 min, and the model vRNA that was not cleaved in the reaction was quantified using qRT-PCR. We found that 72.9% of the model vRNA was not cleaved after

incubation with GZ828PA, whereas 51.5% of the model vRNA was intact after incubation with GZ828PA/V100I (Fig. 6P). We did a similar test with the LN265PA and LN265PA/I100V proteins and found that only 8.6% of the model vRNA was not cleaved after incubation with LN265PA, whereas 54.2% of the model vRNA was intact after incubation with LN265PA/I100V (Fig. 6Q). These results indicate that the mutation V100I in the PA of GZ828 enhances its endonuclease cleavage activity and the mutation I100V in the PA of LN265 reduces its endonuclease cleavage activity.

Discussion

The EA H1N1 swine influenza viruses have been widely detected in pigs in many European and Asian countries and have caused human infections in the Netherlands, Switzerland, Spain, Italy, and China (21–31). The viruses circulating in pigs in China have formed multiple genotypes through reassortment with other swine influenza viruses, and some viruses have become highly lethal in mammals. In this study, we compared two viruses from the same genotype and found that these two viruses have different pathotypes in mice: GZ828 is mild and LN265 is highly lethal in mice. Using reverse genetics, we generated and investigated a series of single-gene reassortants and mutants and identified four amino acids in PA that are responsible for the pathogenicity difference between these two viruses in mice. We further demonstrated that these four amino acids in PA collectively contribute to the disease severity caused by LN265 and its efficient respiratory droplet transmission in ferrets. Moreover, we found that the amino acid mutation V100I in PA enhances its endonuclease cleavage activity and that the mutations N321K and I330V in PA enhance its vRNA-binding ability, thereby revealing the underlying mechanism of the increased pathogenicity and transmissibility of the LN265 virus.

In a previous study, we evaluated the transmission in ferrets of 10 H1N1 swine influenza viruses that bear the HA of the EA H1N1 lineage and found that four of them—three pure EA H1N1 viruses and an EA H1N1 reassortant that derived its six internal genes from the 2009/H1N1 virus—transmitted to all three exposed ferrets (3). Of note, the earliest detection time points of those four viruses in the exposed ferrets ranged from 3 d to 7 d p.e., and these viruses did not kill any mice at a dosage of $10^{6.0}$ EID₅₀ (3). In the present study, GZ828 and LN265 killed all tested mice at a dosage of $10^{6.0}$ EID₅₀ and $10^{3.0}$ EID₅₀, respectively, and LN265 transmitted to all three ferrets as early as 1 d p.e. These findings suggest that the EA H1N1 reassortant LN265 is more lethal in mice and more transmissible in ferrets than the earlier EA H1N1 viruses, thereby posing an increased threat to public health.

The pathogenicity and transmissibility of the influenza virus are influenced by a variety of factors that have not yet been fully revealed. Many amino acid mutations in HA are important for its binding to human-type receptors and thereby increase the transmissibility of influenza viruses (19, 45, 46). The amino acids 292V, 627K, and 701N in PB2 have been shown to play important roles in the transmission of influenza viruses (9, 47–49), and 627K and 701N in PB2 have also been reported to increase the pathogenicity of different avian influenza viruses in mice or ferrets (9, 33, 50). More than 78% of the H7N9 viruses isolated from humans have the E627K mutation in their PB2 (9), and Liang et al. found that the acquisition of this mutation is driven by the low polymerase activity attributed to PA (34). In this study, we found that the EA H1N1 reassortant became highly lethal in mice and transmissible in

ferrets by acquiring more mutations in PA rather than acquiring the 627K mutation in PB2, suggesting that different influenza viruses can acquire the same biological characteristics through different mechanisms. Of note, we analyzed 14,293 H1N1 viruses that were reported between January 2009 and December 2020, including 474 EA H1N1 reassortants, 12,995 2009/H1N1 viruses from humans, and 824 2009/H1N1 viruses from swine (*SI Appendix, Fig. S6*). We found that these four mutations arose and progressively accumulated in the PA gene of 2009/H1N1 viruses circulating in humans since 2011, and that human 2009/H1N1 viruses carrying some or all of these mutations also transmitted to swine and reassorted with the EA H1N1 viruses (*SI Appendix, Figs. S6–S8*). How these mutations in PA affect the replication, pathogenicity, and transmission of the EA H1N1 reassortant viruses in pigs remains to be evaluated, which will further improve our understanding of the risks of the EA H1N1 reassortant viruses.

PA and PB1 enter the nucleus together, and the quality of their cooperation affects the biological characteristics of the virus (51). Zhang et al. 2013 (52) reported that H5N1 hybrid viruses bearing the PA of the 2009/H1N1 virus and the PB1 of the duck H5N1 virus had higher polymerase activity and were more pathogenic than the parental duck H5N1 virus, whereas hybrid viruses bearing the PB1 of 2009/H1N1 and the PA of the duck H5N1 virus had lower polymerase activity and were less pathogenic than the parental duck H5N1 virus. It is clear from our assessment of the polymerase activity and pathogenicity in mice of the different reassortants that the four amino acid mutations in the PA of LN265 identified in this study do not affect the cooperation between PA and PB1 but increase the mRNA transcription of viral proteins by promoting the vRNA-binding and endonuclease cleavage activity of PA. The underlying mechanism involving the A639T mutation in PA remains to be investigated. These results confirm that PA is a multifunction protein that plays important roles in different steps of the influenza virus life cycle.

In summary, we found that the EA H1N1 virus circulating in swine exhibits increased pathogenicity and transmissibility in

mammals, and we further revealed that its accumulated mutations in PA enhance mRNA transcription through different mechanisms and contribute to the harmful properties of the EA H1N1 virus. Our study provides important insights for monitoring field strains with pandemic potential.

Materials and Methods

All experiments with animals were carried out in strict accordance with the recommendations in the Guide for the Care and Use of Laboratory Animals of the Ministry of Science and Technology of the People's Republic of China. The protocols were approved by the Committee on the Ethics of Animal Experiments of the Harbin Veterinary Research Institute (HVRI) of the Chinese Academy of Agricultural Sciences (CAAS). Virus samples were processed in the enhanced biosafety level 2 facility in the HVRI of the CAAS. Our staff wear gloves, N95 masks, and disposable coveralls when working in the facility, and all waste is autoclaved before being removed from the facility. All animal studies were approved by the review board of the HVRI of the CAAS. The detailed methods for this study are provided in *SI Appendix*.

Data Availability. Sequence data have been deposited in "A Global Initiative on Sharing Avian Flu Data" (GISAID, <https://gisaid.org/>) (EPI1987738–EPI1987753) (53).

ACKNOWLEDGMENTS. We thank Susan Watson for editing the manuscript. This work was supported by the National Key Research and Development Program of China (2021YFD1800200), by the Laboratory for Lingnan Modern Agriculture Project (NT2021007), and by the Japan Initiative for Global Research Network on Infectious Diseases from the Japan Agency for Medical Research and Development.

Author affiliations: ^aState Key Laboratory of Veterinary Biotechnology, Harbin Veterinary Research Institute, Chinese Academy of Agricultural Sciences, Harbin 150001, People's Republic of China; ^bGuangdong Laboratory for Lingnan Modern Agriculture, Guangzhou 510642, People's Republic of China; ^cDivision of Virology, Department of Microbiology and Immunology, International Research Center for Infectious Diseases, Institute of Medical Science, University of Tokyo, Tokyo 108-8639, Japan; ^dThe Research Center for Global Viral Diseases, National Center for Global Health and Medicine Research Institute, Tokyo 162-8655, Japan; and ^eInfluenza Research Institute, Department of Pathobiological Sciences, School of Veterinary Medicine, University of Wisconsin-Madison, Madison, WI 53711

Author contributions: F.M., H.Y., Y.K., and H.C. designed research; F.M., H.Y., Z.Q., Y.C., Yijie Zhang, Yaping Zhang, L.L., and X.Z. performed research; F.M., H.Y., C.L., Y.K., and H.C. analyzed data; and F.M. and H.C. wrote the paper.

- D. Vijaykrishna et al., Long-term evolution and transmission dynamics of swine influenza A virus. *Nature* **473**, 519–522 (2011).
- G. S. Freidl et al.; FLURISK Consortium, Influenza at the animal-human interface: A review of the literature for virological evidence of human infection with swine or avian influenza viruses other than A(H5N1). *Euro Surveill.* **19**, 20793 (2014).
- H. Yang et al., Prevalence, genetics, and transmissibility in ferrets of Eurasian avian-like H1N1 swine influenza viruses. *Proc. Natl. Acad. Sci. U.S.A.* **113**, 392–397 (2016).
- H. Sun et al., Prevalent Eurasian avian-like H1N1 swine influenza virus with 2009 pandemic viral genes facilitating human infection. *Proc. Natl. Acad. Sci. U.S.A.* **117**, 17204–17210 (2020).
- R. J. Garten et al., Antigenic and genetic characteristics of swine-origin 2009 A(H1N1) influenza viruses circulating in humans. *Science* **325**, 197–201 (2009).
- E. D. Kilbourne, Influenza pandemics of the 20th century. *Emerg. Infect. Dis.* **12**, 9–14 (2006).
- D. J. Alexander, I. H. Brown, History of highly pathogenic avian influenza. *Rev. Sci. Tech.* **28**, 19–38 (2009).
- Y. Li et al., Continued evolution of H5N1 influenza viruses in wild birds, domestic poultry, and humans in China from 2004 to 2009. *J. Virol.* **84**, 8389–8397 (2010).
- J. Shi et al., H7N9 virulent mutants detected in chickens in China pose an increased threat to humans. *Cell Res.* **27**, 1409–1421 (2017).
- P. Cui et al., Genetic and biological characteristics of the globally circulating H5N8 avian influenza viruses and the protective efficacy offered by the poultry vaccine currently used in China. *Sci. China Life Sci.* **65**, 795–808 (2021).
- X. Zeng et al., Vaccination of poultry successfully eliminated human infection with H7N9 virus in China. *Sci. China Life Sci.* **61**, 1465–1473 (2018).
- World Organisation for Animal Health, Avian influenza weekly update. https://www.who.int/docs/default-source/wpro-documents/emergency-surveillance/avian-influenza/ai-20220204.pdf?sfvrsn=223ca73f_183. Accessed 24 February 2022.
- J. Shi et al., Rapid evolution of H7N9 highly pathogenic viruses that emerged in China in 2017. *Cell Host Microbe* **24**, 558–568.e7 (2018).
- M. Pensaert, K. Ottis, J. Vandeputte, M. M. Kaplan, P. A. Bachmann, Evidence for the natural transmission of influenza A virus from wild ducks to swine and its potential importance for man. *Bull. World Health Organ.* **59**, 75–78 (1981).
- T. Ito et al., Molecular basis for the generation in pigs of influenza A viruses with pandemic potential. *J. Virol.* **72**, 7367–7373 (1998).
- R. E. Shope, Swine influenza: I. Experimental transmission and pathology. *J. Exp. Med.* **54**, 349–359 (1931).
- T. K. Anderson et al., A phylogeny-based global nomenclature system and automated annotation tool for H1 hemagglutinin genes from swine influenza A viruses. *mSphere* **1**, e00275-16.
- G. Neumann, T. Noda, Y. Kawaoka, Emergence and pandemic potential of swine-origin H1N1 influenza virus. *Nature* **459**, 931–939 (2009).
- Y. Zhang et al., Key molecular factors in hemagglutinin and PB2 contribute to efficient transmission of the 2009 H1N1 pandemic influenza virus. *J. Virol.* **86**, 9666–9674 (2012).
- A. Vincent et al., Review of influenza A virus in swine worldwide: A call for increased surveillance and research. *Zoonoses Public Health* **61**, 4–17 (2014).
- G. F. Rimmelzwaan et al., Antigenic and genetic characterization of swine influenza A (H1N1) viruses isolated from pneumonia patients in The Netherlands. *Virology* **282**, 301–306 (2001).
- J. F. Xie et al., Emergence of Eurasian avian-like swine influenza A (H1N1) virus from an adult case in Fujian province, China. *Viol. Sin.* **33**, 282–286 (2018).
- P. L. A. Fraaij et al., Severe acute respiratory infection caused by swine influenza virus in a child necessitating extracorporeal membrane oxygenation (ECMO), the Netherlands, October 2016. *Euro Surveill.* **21**, 30416 (2016).
- X. Li et al., Human infection with a novel reassortant Eurasian-avian lineage swine H1N1 virus in northern China. *Emerg. Microbes Infect.* **8**, 1535–1545 (2019).
- W. Zhu et al., Reassortant Eurasian avian-like influenza A(H1N1) virus from a severely ill child, Hunan Province, China, 2015. *Emerg. Infect. Dis.* **22**, 1930–1936 (2016).
- H. Yang et al., Human infection from avian-like influenza A (H1N1) viruses in pigs, China. *Emerg. Infect. Dis.* **18**, 1144–1146 (2012).
- D. Y. Wang et al., Human infection with Eurasian avian-like influenza A(H1N1) virus, China. *Emerg. Infect. Dis.* **19**, 1709–1711 (2013).
- A. Parys et al., Human infection with Eurasian avian-like swine influenza A(H1N1) virus, The Netherlands, September 2019. *Emerg. Infect. Dis.* **27**, 939–943 (2021).
- X. Qi et al., Antigenic and genetic characterization of a European avian-like H1N1 swine influenza virus from a boy in China in 2011. *Arch. Virol.* **158**, 39–53 (2013).
- V. Gregory et al., Human infection by a swine influenza A(H1N1) virus in Switzerland. *Arch. Virol.* **148**, 793–802 (2003).
- F. Rovida et al., Swine influenza A (H1N1) virus (SIV) infection requiring extracorporeal life support in an immunocompetent adult patient with indirect exposure to pigs, Italy, October 2016. *Euro Surveill.* **22**, 30456 (2017).

32. H. Li *et al.*, Prevalence, genetics and evolutionary properties of Eurasian avian-like H1N1 swine influenza viruses in Liaoning. *Viruses* **14**, 643 (2022).
33. Z. Li *et al.*, Molecular basis of replication of duck H5N1 influenza viruses in a mammalian mouse model. *J. Virol.* **79**, 12058–12064 (2005).
34. L. Liang *et al.*, Low polymerase activity attributed to PA drives the acquisition of the PB2 E627K mutation of H7N9 avian influenza virus in mammals. *MBio* **10**, e01162-19 (2019).
35. Q. Zhang *et al.*, H7N9 influenza viruses are transmissible in ferrets by respiratory droplet. *Science* **341**, 410–414 (2013).
36. J. Shi *et al.*, Susceptibility of ferrets, cats, dogs, and other domesticated animals to SARS-coronavirus 2. *Science* **368**, 1016–1020 (2020).
37. S. S. Lakdawala *et al.*, The soft palate is an important site of adaptation for transmissible influenza viruses. *Nature* **526**, 122–125 (2015).
38. A. J. Te Velthuis, E. Fodor, Influenza virus RNA polymerase: Insights into the mechanisms of viral RNA synthesis. *Nat. Rev. Microbiol.* **14**, 479–493 (2016).
39. A. R. Dawson *et al.*, Phosphorylation controls RNA binding and transcription by the influenza virus polymerase. *PLoS Pathog.* **16**, e1008841 (2020).
40. J. Li *et al.*, Viral RNA-binding ability conferred by SUMOylation at PB1 K612 of influenza A virus is essential for viral pathogenesis and transmission. *PLoS Pathog.* **17**, e1009336 (2021).
41. E. Fodor *et al.*, A single amino acid mutation in the PA subunit of the influenza virus RNA polymerase inhibits endonucleolytic cleavage of capped RNAs. *J. Virol.* **76**, 8989–9001 (2002).
42. A. P. Walker, J. Sharps, E. Fodor, Mutation of an influenza virus polymerase 3' RNA promoter binding site inhibits transcription elongation. *J. Virol.* **94**, e00498-20 (2020).
43. K. Hara, F. I. Schmidt, M. Crow, G. G. Brownlee, Amino acid residues in the N-terminal region of the PA subunit of influenza A virus RNA polymerase play a critical role in protein stability, endonuclease activity, cap binding, and virion RNA promoter binding. *J. Virol.* **80**, 7789–7798 (2006).
44. A. Dias *et al.*, The cap-snatching endonuclease of influenza virus polymerase resides in the PA subunit. *Nature* **458**, 914–918 (2009).
45. T. M. Tumpey *et al.*, A two-amino acid change in the hemagglutinin of the 1918 influenza virus abolishes transmission. *Science* **315**, 655–659 (2007).
46. Y. Zhang *et al.*, Pandemic threat posed by H3N2 avian influenza virus. *Sci. China Life Sci.* **64**, 1984–1987 (2021).
47. S. Herfst *et al.*, Airborne transmission of influenza A/H5N1 virus between ferrets. *Science* **336**, 1534–1541 (2012).
48. H. Kong *et al.*, Identification of key amino acids in the PB2 and M1 proteins of H7N9 influenza virus that affect its transmission in guinea pigs. *J. Virol.* **94**, e01180-19 (2019).
49. Y. Gao *et al.*, Identification of amino acids in HA and PB2 critical for the transmission of H5N1 avian influenza viruses in a mammalian host. *PLoS Pathog.* **5**, e1000709 (2009).
50. M. Hatta, P. Gao, P. Halfmann, Y. Kawaoka, Molecular basis for high virulence of Hong Kong H5N1 influenza A viruses. *Science* **293**, 1840–1842 (2001).
51. E. Fodor, M. Smith, The PA subunit is required for efficient nuclear accumulation of the PB1 subunit of the influenza A virus RNA polymerase complex. *J. Virol.* **78**, 9144–9153 (2004).
52. Y. Zhang *et al.*, H5N1 hybrid viruses bearing 2009/H1N1 virus genes transmit in guinea pigs by respiratory droplet. *Science* **340**, 1459–1463 (2013).
53. F. Meng *et al.*, Sequence data in "A Global Initiative on Sharing Avian Flu Data," accession #s EPI1987738–EPI1987753. GISAID. <https://gisaid.org/>. Accessed 3 August 2022.